Monitoring the HRC-S Gain with the LETG/HRC-S

Deron Pease & Jeremy Drake
October 2003

ABSTRACT

We present *Chandra* LETG/HRC-S in-flight gain monitoring data for the HRC-S, acquired from November 1999 through July 2003. For calibration and monitoring purposes the LETG/HRC-S combination has repeatedly observed HZ 43 and PKS 2155-304. These data show that since LETGS in-flight calibration began the median PHA has dropped by $23-28\%$ at the nominal aimpoint, by an average of 12% along the LETG dispersion line on the central MCP, and by an average of 19% along the dispersion line on the wing MCPs. The bulk of the drop occurred within the first months of the mission, with a subsequently smaller median PHA drop of $\lesssim$10%. Current simple rate-of-decay models predict that a 5% loss of source events due to PHA drop alone is expected in $\gtrsim 10$ years from October 2003.

1. INTRODUCTION

As part of the *Chandra* in-flight calibration program, beginning in fall 1999 AR Lac has been observed regularly by the HRC-S in imaging mode to spot-check the gain over a pattern which covers some of the HRC-S central microchannel plate (MCP). (See *CXC* Memo by Posson-Brown & Donnelly (2003) detailing the HRC imaging-mode gain monitoring). Also ongoing for in-flight calibration, the LETG/HRC-S instrument combination (LETGS) has been used to observe HZ 43 and PKS 2155-304 in order to calibrate and monitor various performance issues, primarily quantum efficiency and effective area. In this paper, we employ these two sources to study gain evolution by extracting pulse-height amplitude (PHA) distributions and monitoring the median PHA. We chop up LETGS dispersed spectra to monitor HRC-S MCP gain along the nominal dispersion line. Thus, gain trends are studied both temporally and spatially.

2. OBSERVATIONS AND DATA REDUCTION

HZ 43 and PKS 2155-304 were observed 7 and 6 times, respectively, by the LETGS between November 1999 and July 2003 (see Table 1). The LETGS dispersion of HZ 43 provides good coverage on the HRC-S wing MCPs only, while the spectrum of PKS 2155-304 is confined to the central MCP. Unfortunately, there is no usable overlap between the two sources.

Both L1 event lists, for which only the highest pulse-height channel was filtered out (PHA=255), and L2 event lists, with the low-impact ($<1\%$ source events) LETGS PI background filtering scheme applied (Wargelin et al. 2001), were analyzed and produced the same results. (In part, this study is also a test of the PI filtering scheme). Data were analyzed in (DETX,DETY) coordinates to define the detector space covered by the dither pattern, and to facilitate the making of regions. The outer MCPs (HZ 43 dispersed data) were chopped up into 12 regular box bins, each about 10Å long and wide enough to enclose the dispersed source events. The central MCP (PKS 2155-304 data) was chopped into 11 box bins of the same size, omitting a box around the aimpoint. For the aimpoint study of both sources, a box just around the 0th order dither pattern was used. All bins had statistics better than 3%. Figure 1 shows an example of bin regions in (DETX,DETY) coordinates.

Table 1. Summary of LETG+HRC-S Calibration Observations

Source	Obs ID	UT Start	Exposure (s)
HZ 43	59	1999-11-12 04:32:08	39798
	1011	2001-03-18 21:50:28	18653
	1012	2001-08-18 13:57:23	19947
	2584	2002-01-01 19:51:46	19003
	2595	2002-07-23 14:01:38	19989
	3676	2002-12-04 23:24:07	19842
	3677	2003-07-24 03:24:43	20009
PKS 2155-304	331	1999-12-25 13:17:02	62658
	1704	2000-05-31 09:42:14	25835
	1013	2001-04-06 14:39:52	26643
	3166	2001-11-30 02:23:40	29771
	3709	2002-11-30 14:48:28	13749
	4406	2002-11-30 21:06:05	13850

Note: the two most recent observations of PKS 2155-304 (ObsIDs 3709 and 4406) were intended as a single observation and, therefore, were combined for this analysis.

Event PHAs were extracted to create a PHA distribution for each bin. The evolution of the PHA distributions was monitored by computing the median PHA for each distribution. In addition to these values derived empirically from the data, we made least-squares fits of Gaussian functions to the PHA distributions, for qualitative study only. The Gaussian shape does not ideally represent the data; however, we find that it is adequate for monitoring trends. The Gaussian coefficients were not relied on quantitatively.

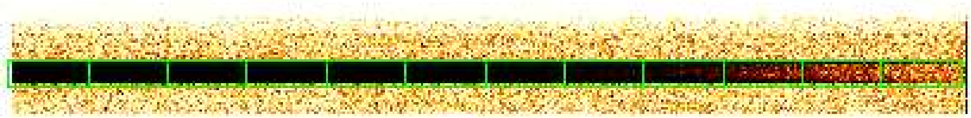

Figure 1. Example of PHA extraction bins for LETGS dispersion. HZ 43 (ObsID 59) negative dispersion MCP.

3. RESULTS

HZ 43 and PKS 2155-304 data both show a total drop in median PHA of $\sim 23 - 28\%$ to date. They also both appear to indicate that a large drop of $\sim 15\%$ took place early in the mission, relative to the subsequent downward trend ($\sim 8 - 11\%$) over the last 2−3 years. (Note: Due to lack of room on the following PHA plots and redundancy of the scheme, unless otherwise stated, the color and symbol key for plots within this paper is presented in Figure 2).

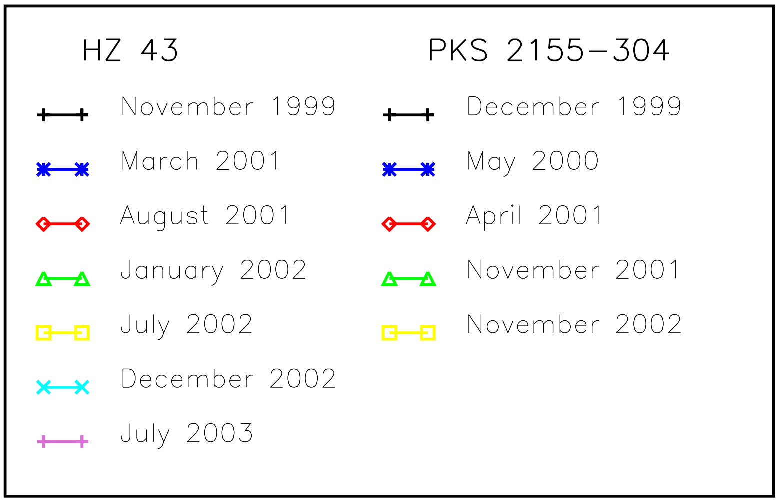

Figure 2. Legend for Figures 3−12 and 14.

HZ 43 aimpoint data show a $\sim$ 28% total drop in median PHA since the first observation in November 1999, but only $<$ 8% drop since March 2001 (see Figures 3−4). To further study the downward trends, we modeled the aimpoint data by making 1) an exponential fit to the full data set and 2) a linear fit to the data excluding the first observation. The model curves, shown overplotted on Figure 3, can be used to quantify and perhaps to predict gain evolution.

The HZ 43 data dispersed onto the wing MCPs show an average 19% total drop since November 1999 and 8% drop subsequently (see Figures 5−8). Note also that it is possibly interesting that each wing MCP exhibits the same basic median PHA shape across the plates in the same direction (for example, in DETX space). This effect could indicate amplifier behavior, since both plates share the same amplifiers.

The PKS 2155-304 aimpoint data show a 23% total drop since December 1999, but only 11% since May 2000 (see Figures 9−10). As with HZ 43, the PKS 2155-304 aimpoint data were modeled by 1) an exponential fit to the full data set and 2) a linear fit to the data excluding the first observation. In this case, however, there are fewer observations with which to constrain the models, resulting in larger uncertainties in the curves and their interpretations.

Elsewhere on the central MCP we find an average 12% total drop, with an average of 8% subsequently (see Figures 11−12). Also note in Figure 11 that the aimpoint is depressed significantly relative to neighboring bins. This may be evidence for the “hole” possibly inflicted in the HRC-S at XRCF.

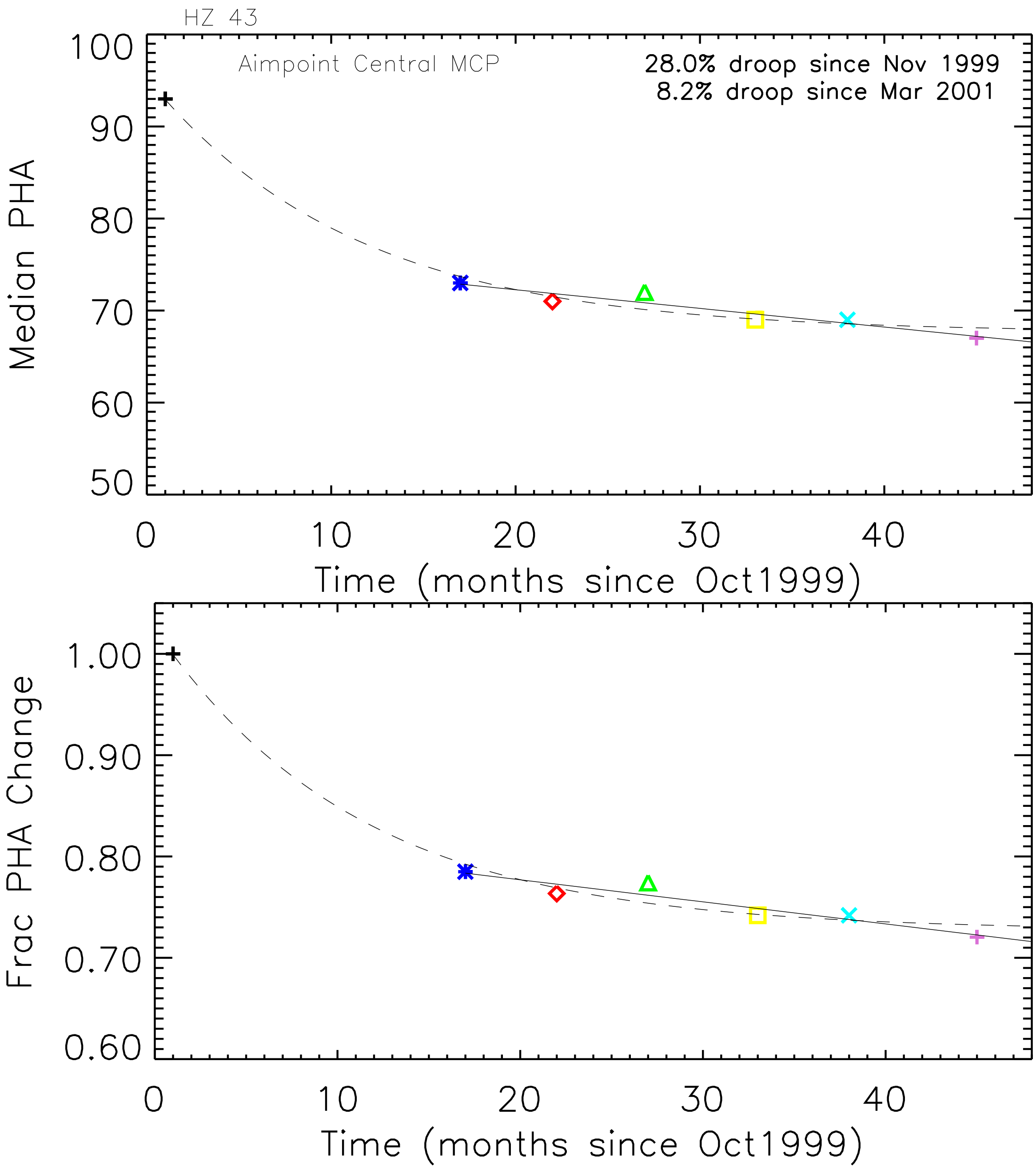

Figure 3. HZ 43 aimpoint median PHA evolution, with exponential (dashed curve) and linear (solid line) fits (see text). Bottom plot normalized to the first observation, ObsID 59.

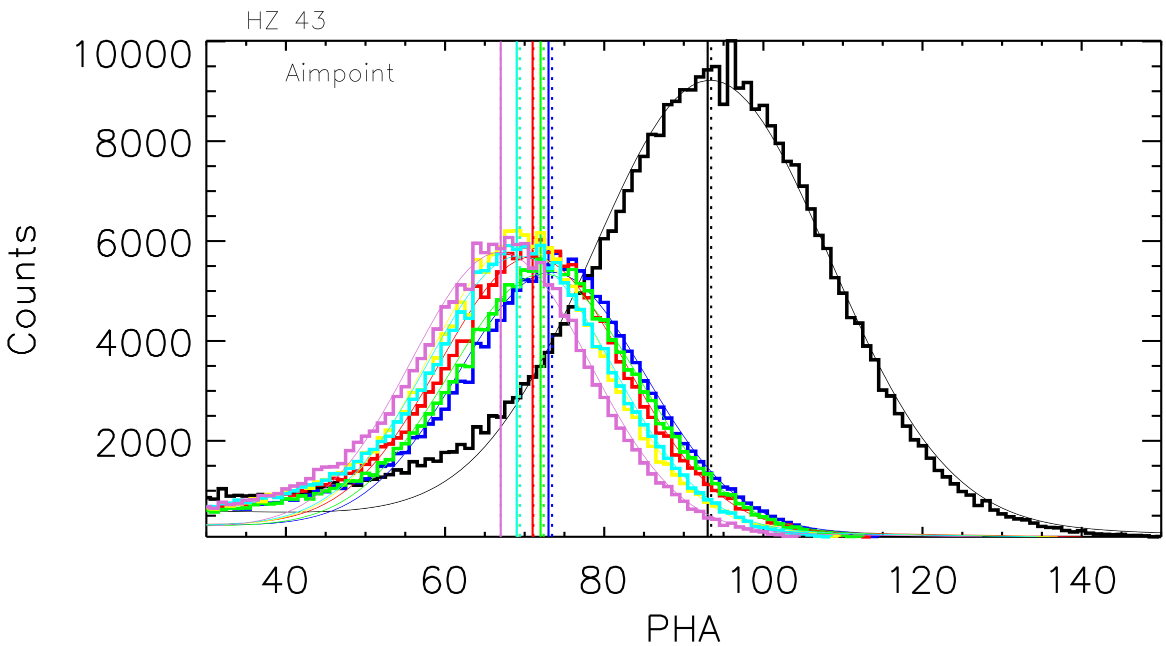

Figure 4. HZ 43 aimpoint PHA distribution. Solid vertical lines mark the median PHA. Gaussian fits overplotted. Note: total counts vary in accordance with differing exposure times per observation.

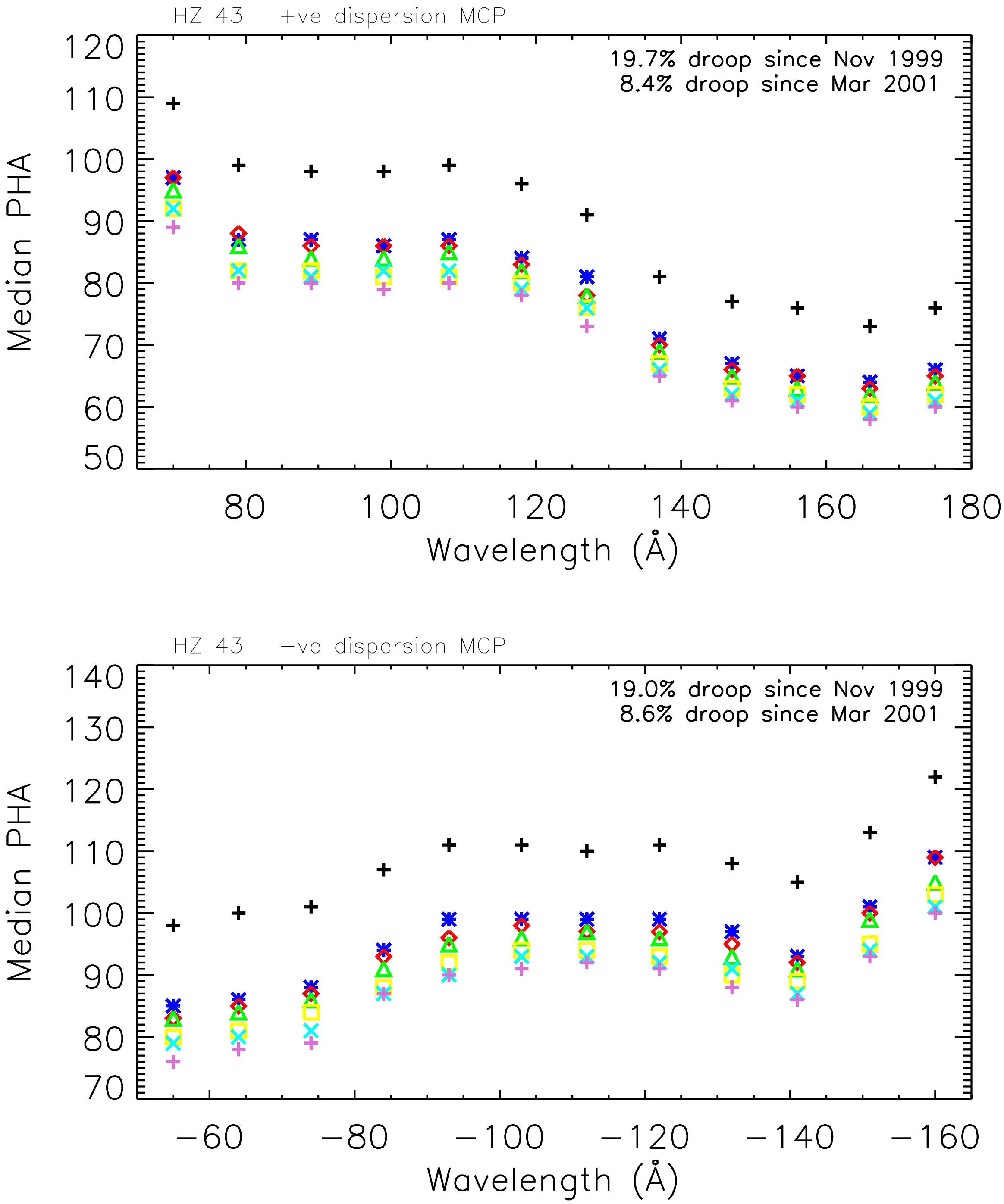

Figure 5. HZ 43 median PHA evolution for the 12 dispersion bins on each of the wing MCPs. Top plot: positive dispersion MCP. Bottom plot: negative dispersion MCP.

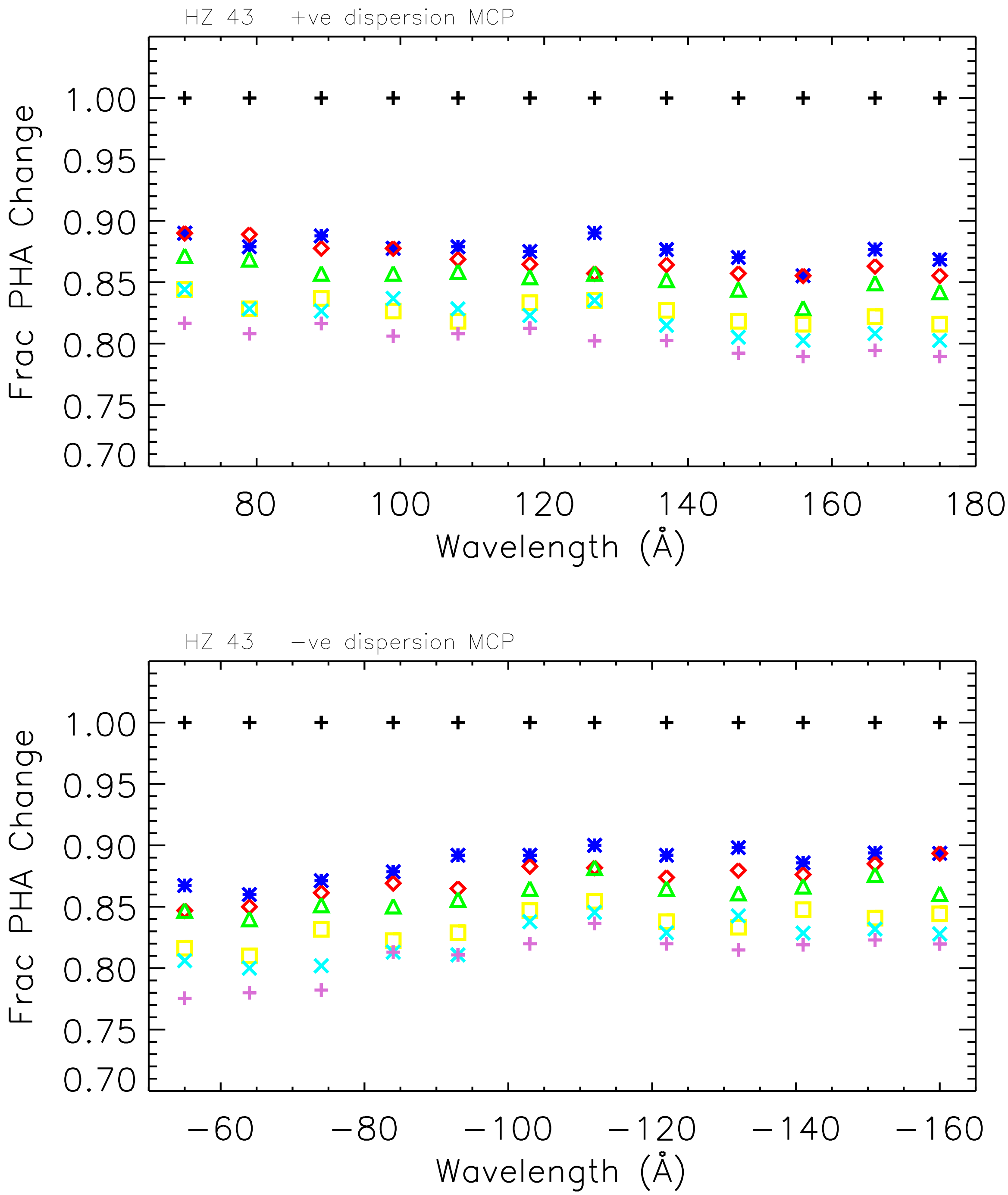

Figure 6. HZ 43 median PHA evolution (data as in Figure 5), normalized to ObsID 59. Top plot: positive dispersion MCP. Bottom plot: negative dispersion MCP.

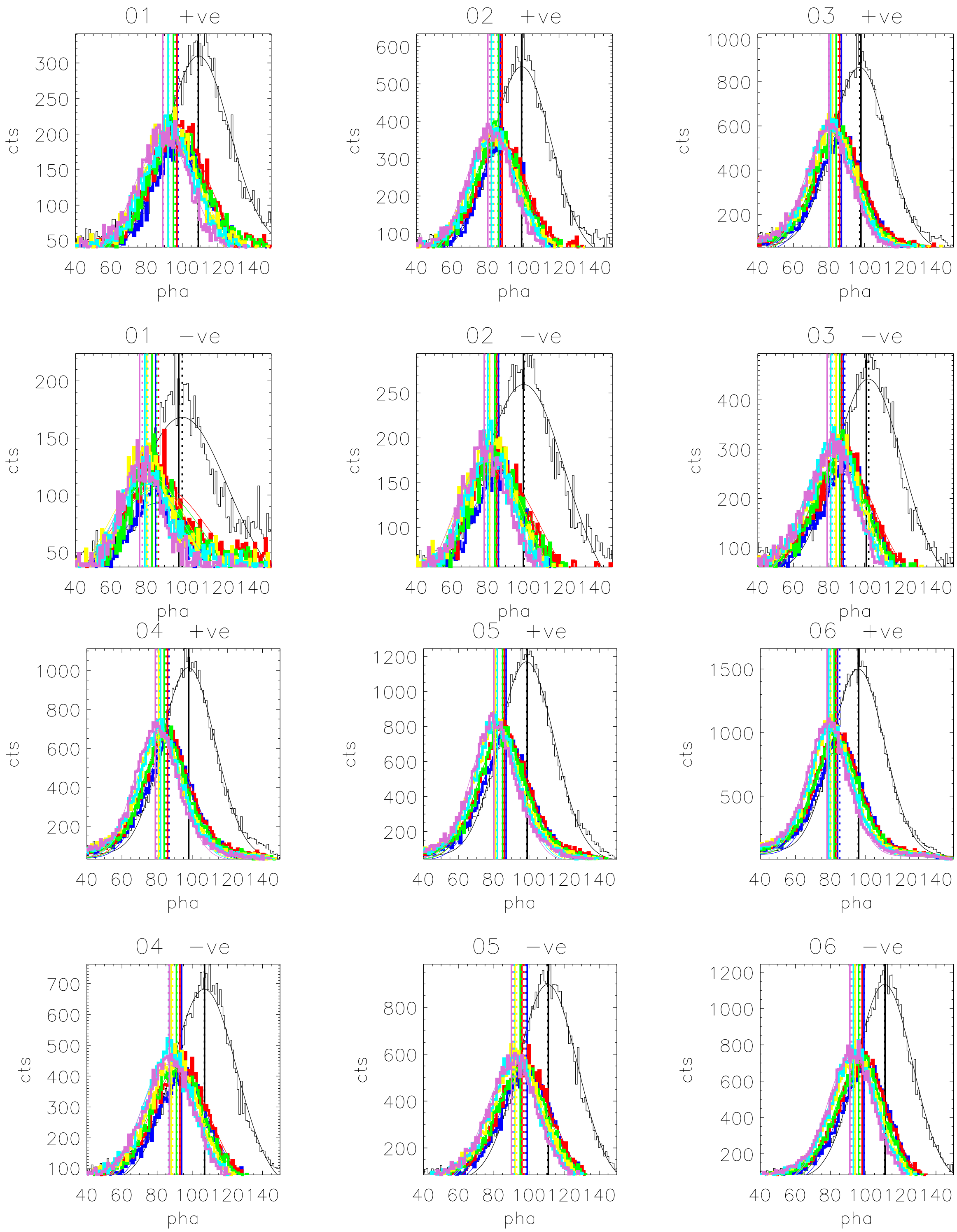

Figure 7. HZ 43 wing MCP PHA distributions. Solid vertical lines mark the median PHA. Gaussian fits overplotted. Bin numbers increase from center outward on MCPs. Positive and negative MCP bins plotted on alternating rows to facilitate comparison. Bins 01−06.

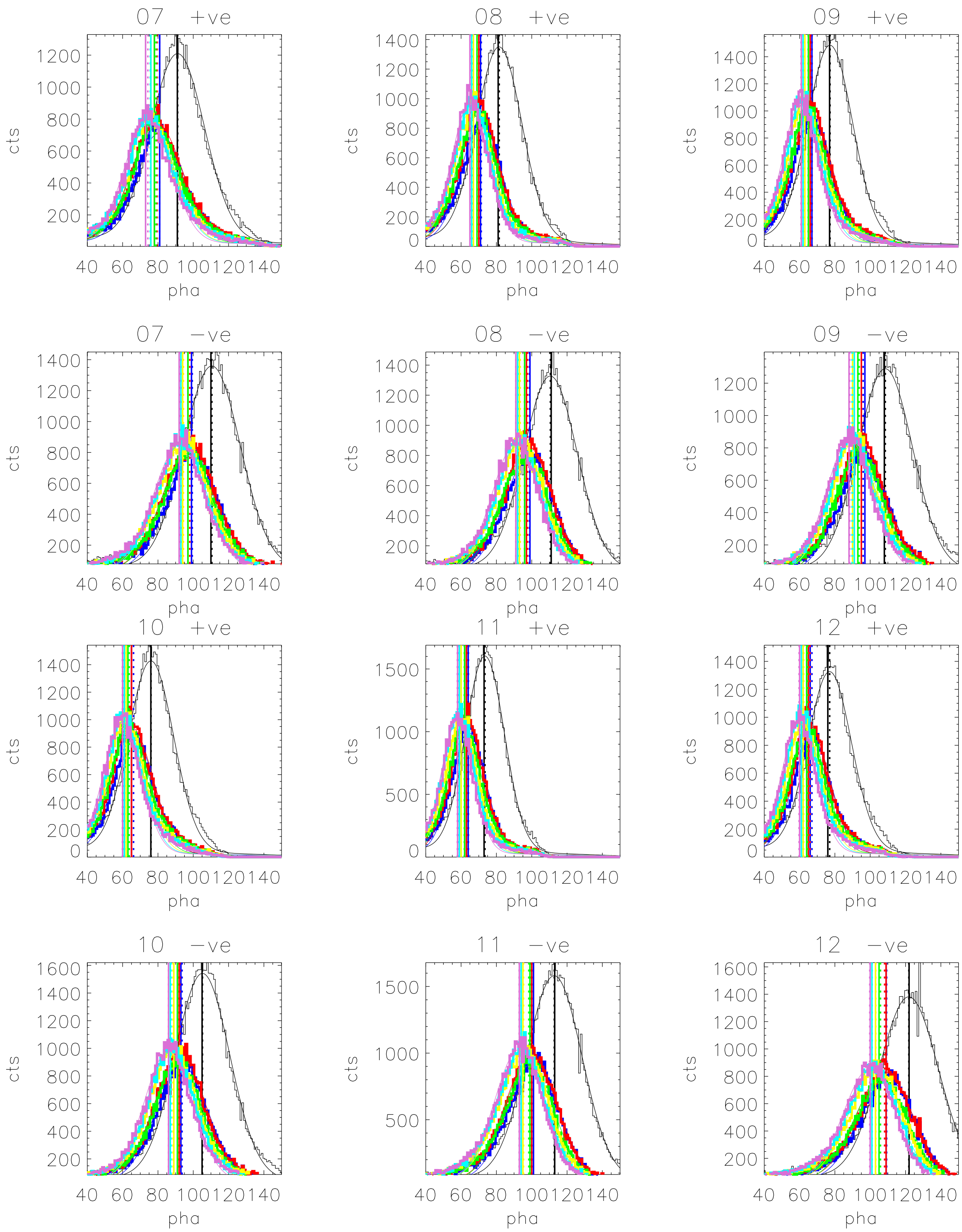

Figure 8. As in Figure 7. Bins 07−12.

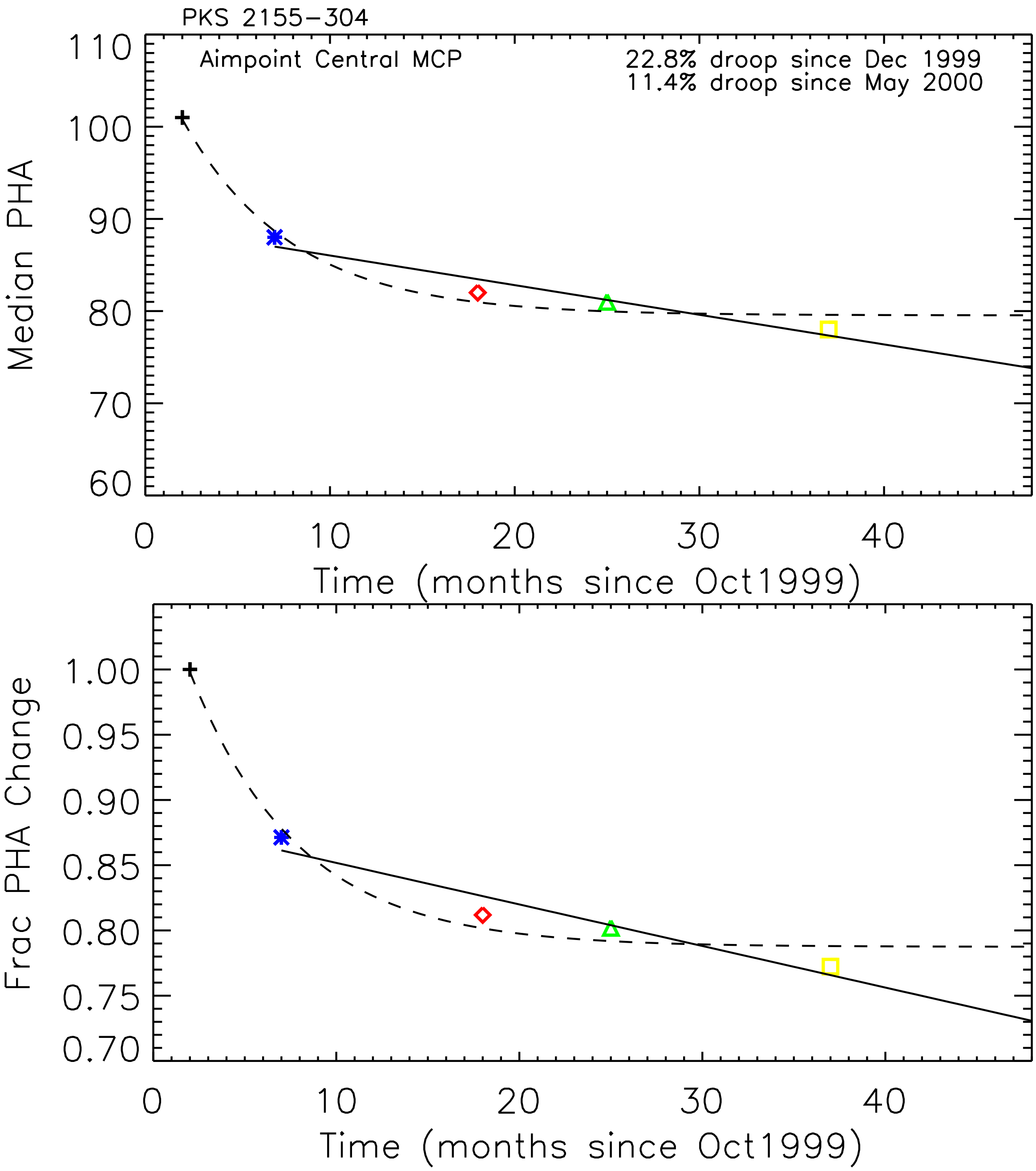

Figure 9. PKS 2155-304 aimpoint median PHA evolution, with exponential (dashed curve) and linear (solid line) fits (see text). Bottom plot normalized to first observation, ObsID 331.

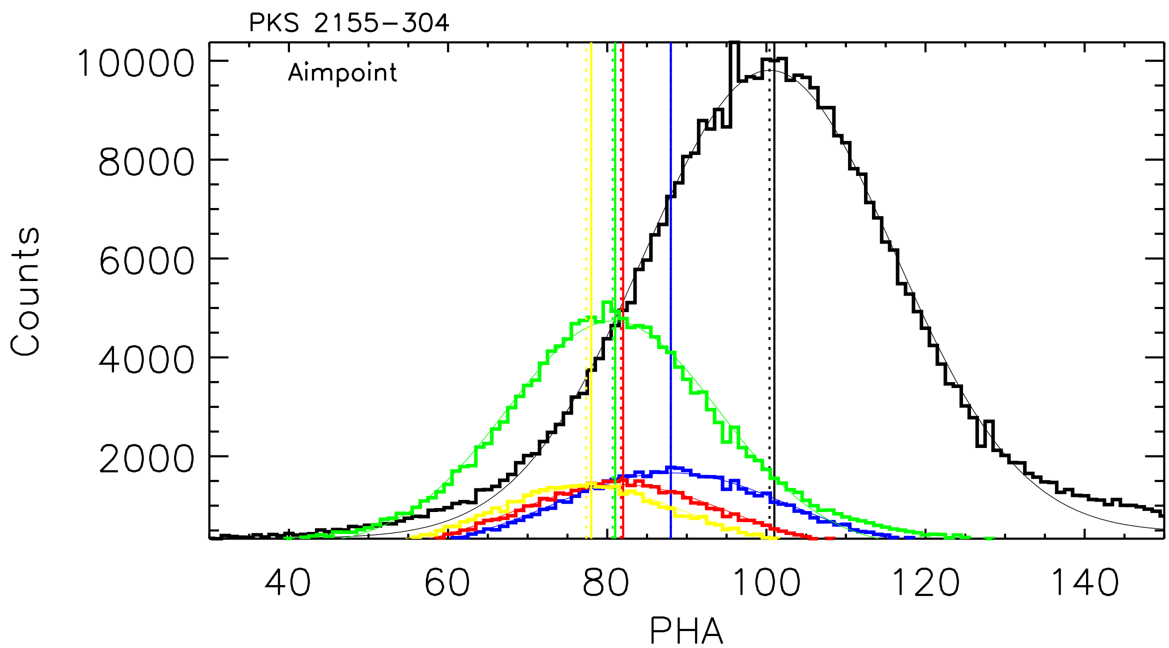

Figure 10. PKS 2155-304 aimpoint PHA distribution. Solid vertical lines mark the median PHA. Gaussian fits overplotted. Note: total counts vary in accordance with intrinsic source variability and differing exposure times per observation.

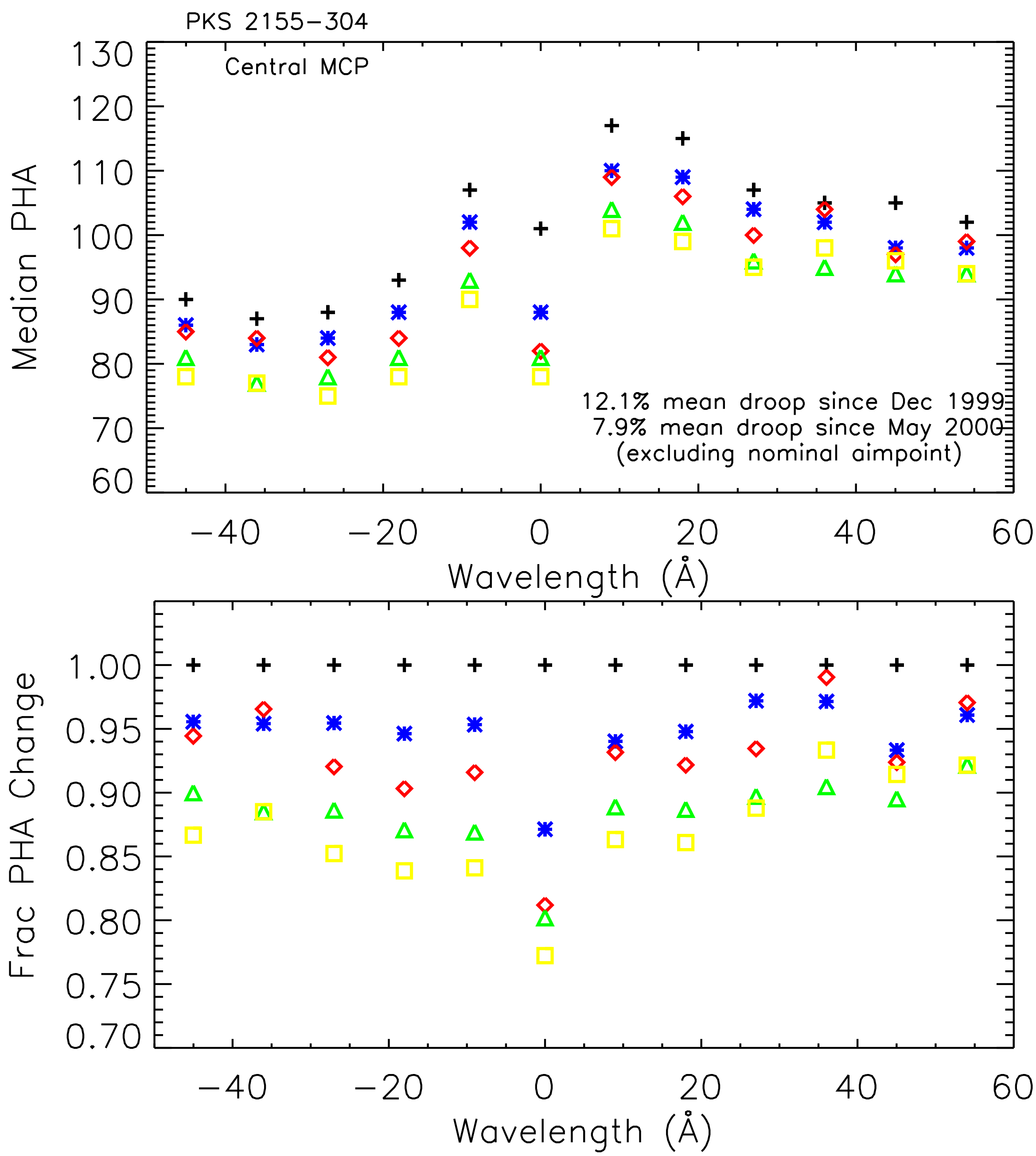

Figure 11. PKS 2155-304 median PHA evolution for the 11 dispersion bins (5 negative, 6 positive) on the central MCP. Aimpoint data plotted for comparison. Note the depression at 0th order (aimpoint). Bottom plot normalized to ObsID 331.

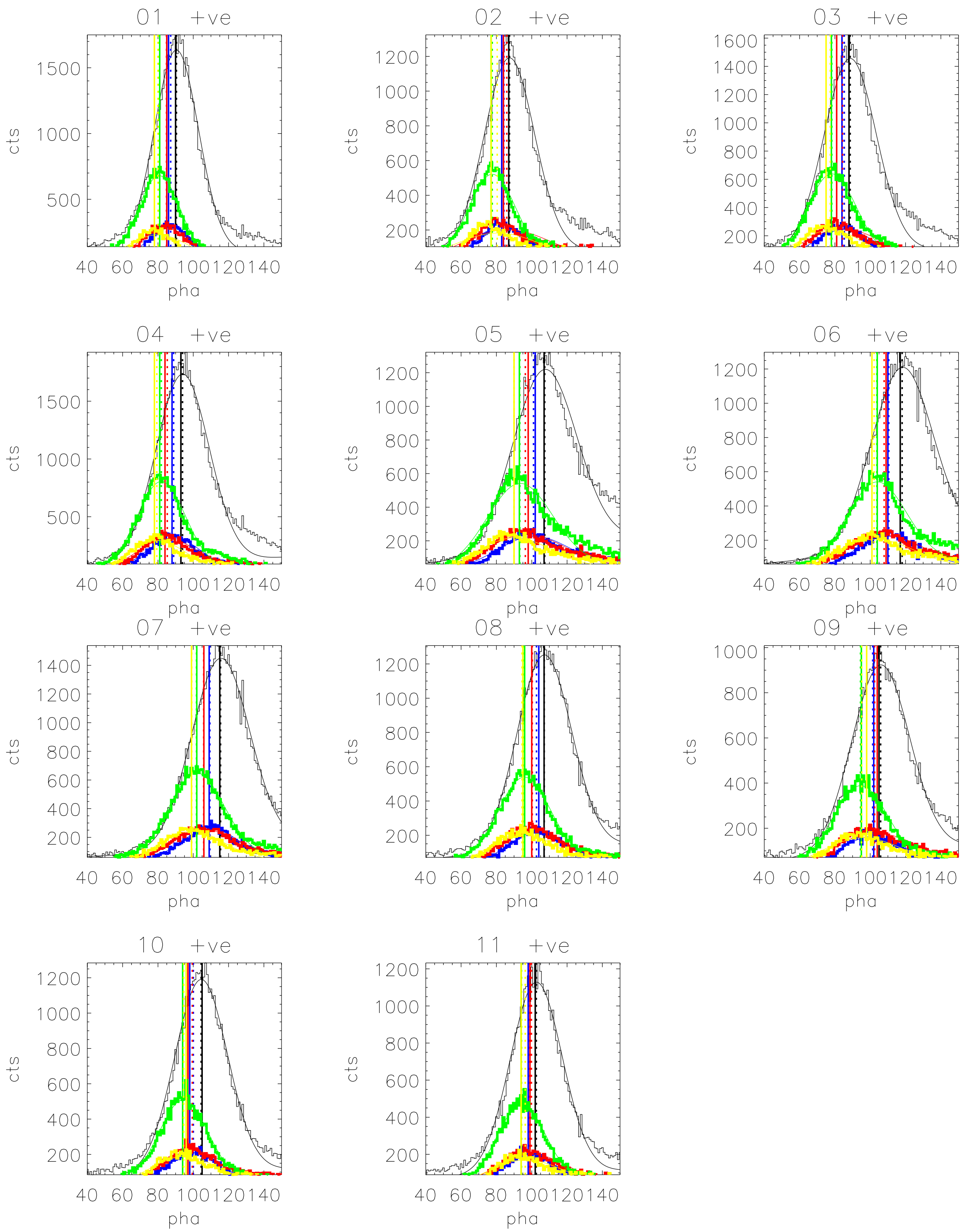

Figure 12. PKS 2155-304 central MCP PHA distributions. Solid vertical lines mark the median PHA. Gaussian fits overplotted. Bin numbers increase across central MCP from negative to positive, skipping over aimpoint.

4. SUMMARY, COMMENTARY & IMPLICATIONS

From two independent sources monitored on a regular basis the aimpoint data imply that the bulk of the median PHA drop ($\sim 15\%$) occurred within the first 5 months of the mission, and possibly in a shorter time. The drop in median PHA was $\lesssim$10% over the subsequent, much longer time of 2–3 years. Current expectations are for the decline to continue at this lower rate.

As the downward trend continues, the source PHA distribution will eventually sag below the lower level discriminator (LLD) and source events will be lost. The HRC-S LLD is currently set to a PHA value of 8. By extrapolating our linear fits to the aimpoint data, and assuming the overall shape of the PHA distribution remains stable, we find that a 5% loss in source events due to PHA evolution alone is expected in 10–13 years from October 2003. This result is somewhat dependent on the source spectrum. HZ 43 presumably presents the worst case since it is the softest source with lowest median PHA values available for study.

In Figure 13, we combine the aimpoint data from HZ 43 and PKS 2155-304 and add AR Lac* and Capella†. As before, we derive exponential and linear models to describe PHA evolution. The linear model fit to the combined data suggests that a 5% loss in source events is expected in ~15 years.

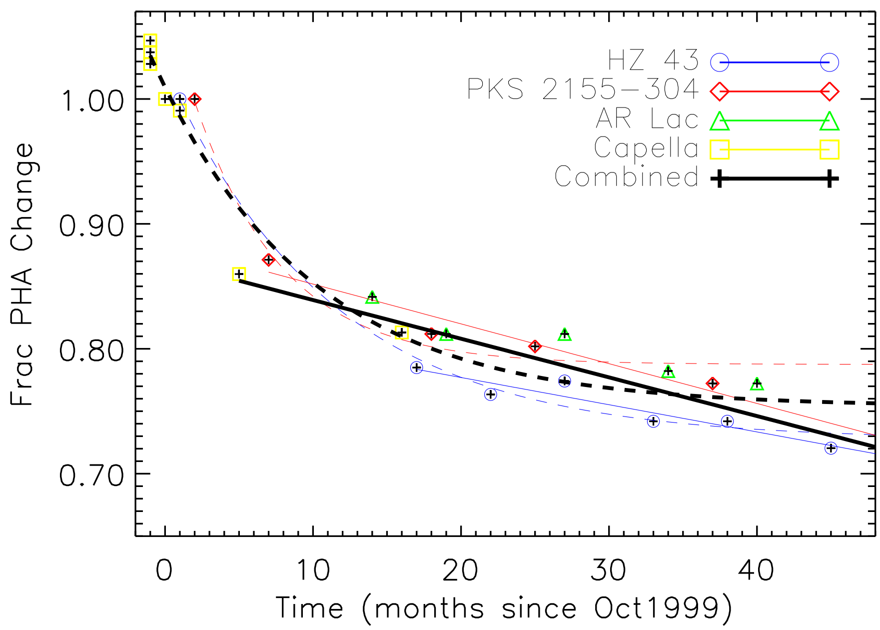

Figure 13. Aimpoint data for HZ 43 (blue), PKS 2155-304 (red), and Combined (HZ 43, PKS 2155-304, AR Lac and Capella – black), with exponential (dashed curve) and linear (solid line) fits to model PHA evolution. All observations are normalized to November/December 1999.

Before events fall below the LLD, the PHA distribution down-shift may cause source events to be removed by the LETGS PI background filter. As a result, the PI filtering scheme may have to be adjusted in the future, though the "light filter" (typically recommended to users) appears to not be rejecting source events, yet. The light filter PI values range from $\sim 20-35$, and translate roughly to PHA values of $\sim 10-20$. Applying the aimpoint rate-of-decline models (used for above predictions)

*AR Lac PHA data from Posson-Brown & Donnelly (2003)

†Capella ObsIDs 62435, 1167, 1244, 1246, 1420, 1248, 58, 1009

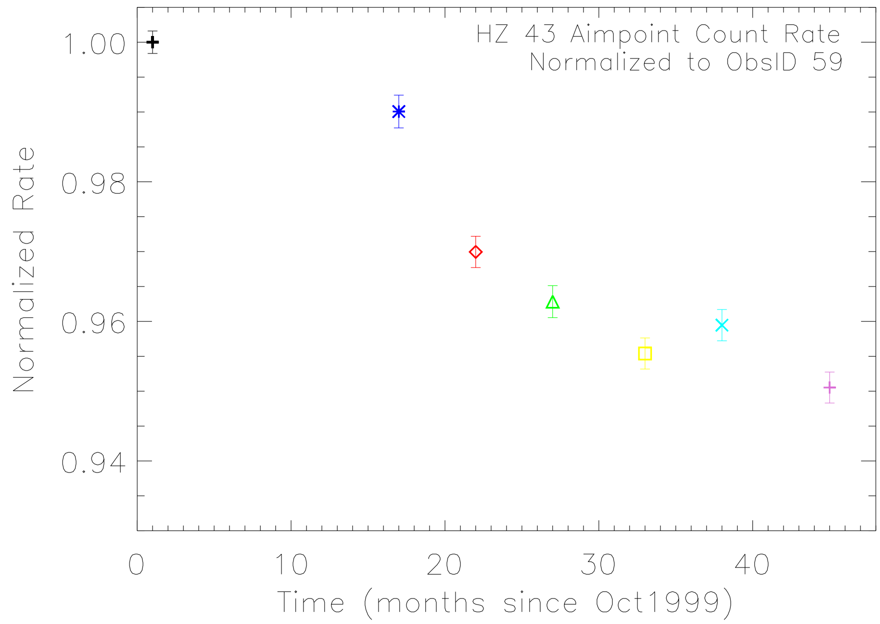

Figure 14. Evidence for QE degradation? HZ 43 aimpoint count rate evolution shows downward trend. Normalized to first observation, ObsID 59. Error bars represent statistical error of each observation only.

we find that the light PI filter would cause a 5% loss in source events in 8−11 years from October 2003. This result is somewhat dependent on detector location as the gain varies over the HRC-S. However, the actual expected rates-of-decline along the line of dispersion appear to be lower than that for the aimpoint. Thus, assuming current trends continue, the aimpoint values are lower limits and the lifetime before significant source event loss will be longer.

The loss of source events will manifest itself in a lowering of detector quantum efficiency (QE). Currently, the HRC-S source PHA distribution is narrow enough and far enough above the LLD to avoid loss of source events. However, LETGS QE studies of HZ 43 have shown that the QE along the line of dispersion appears to have decreased by 2−3% (Drake et al. 2002), while there is evidence for a drop in QE of ∼5% at the nominal aimpoint (see Figure 14). To date, we find that PHA evolution at the aimpoint has resulted in $\ll 1\%$ loss of events. Figures 15 and 16 show the LLD and light PI filter cut-offs and their insignificant impacts. This result implies that the PHA drop is not responsible for the drop in QE witnessed. An alternative possibility to PHA drop is that the QE deficit may indicate that the HRC-S is entering countrate non-linearity, temporarily depressing the QE for bright sources. HZ 43 has a very high countrate in the LETGS of ~ 10 ct s^{-1}. Furthermore, the consistent downward trend would imply that countrate non-linearity worsens over time. The problem with testing this theory is that other than HZ 43 we have not observed any non-variable sources regularly over the lifetime of the mission. Additionally, there are other considerations with the HRC-S such as double-counting (Juda 2002). The cause for the QE degradation is still under investigation.

In conclusion, while there is no immediate need to correct for the HRC-S gain droop, this study and that by Posson-Brown & Donnelly (2003) have opened up discussion. Impacts on LETG calibration and science caused by adjustments made to the instrument gain must be considered. Meanwhile, we continue to monitor HRC-S gain and QE with LETGS observations.

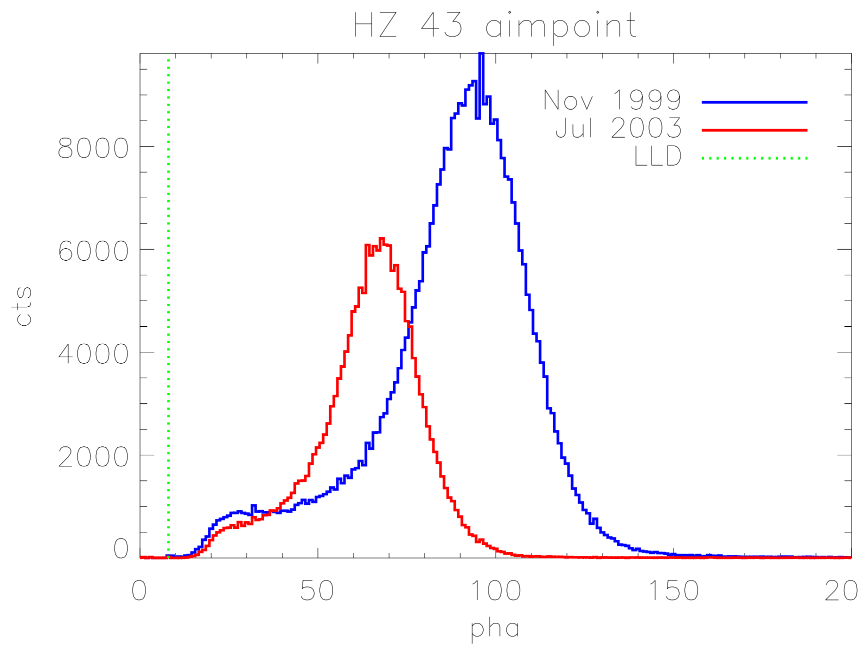

Figure 15. HZ 43 aimpoint PHA distribution for November 1999 (first) and July 2003 (most recent) observations, and the $\ll 1\%$ impact of the LLD.

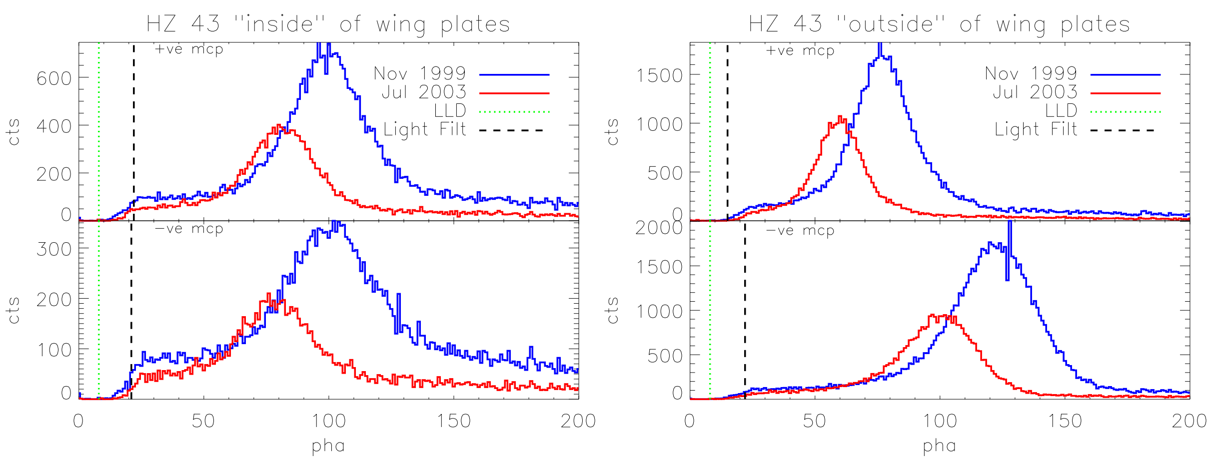

Figure 16. HZ 43 wing plate PHA distributions for November 1999 and July 2003 observations, and the $\ll 1\%$ impact of the LLD and light PI filter cut-offs. Note: total counts vary in accordance with differing exposure times per observation.

REFERENCES

1. Drake, J., et al. 2002, CXC Calibration Workshop
   `http://cxc.harvard.edu/ccw/proceedings/02_proc/`
2. Juda, M. 2002, CXC Memo: HRC-S Double Pulse Fraction
3. Posson-Brown, J. & Donnelly, R.H. 2003, CXC Memo: Evolution of PHA Response in the HRC
4. Wargelin, B., et al. paper in preparation
   `http://cxc.harvard.edu/cal/Letg/Hrc_bg/`